A 260×274 μm² 572 nW Neural Recording Micromote Using Near-Infrared Power Transfer and an RF Data Uplink

Gabriele Atzeni[1], Jongyup Lim[2], Jiawei Liao[1], Alessandro Novello[1], Jungho Lee[2], Eunseong Moon[2], Michael Barrow[2], Joseph Letner[2], Joseph Costello[2], Samuel R. Nason[2], Paras R. Patel[2], Parag G. Patil[2], Hun-Seok Kim[2], Cynthia A. Chestek[2], Jamie Phillips[2,3], David Blaauw[2], Taekwang Jang[1]
[1]ETH Zurich, Zurich, Switzerland, [2]University of Michigan, Ann Arbor, USA and [3]University of Delaware, Newark, USA (email: gatzeni@iis.ee.ethz.ch)

2022 IEEE Symposium on VLSI Technology and Circuits (VLSI Technology and Circuits) | 978-1-6654-9772-5/22/$31.00 ©2022 IEEE | DOI: 10.1109/VLSITechnologyandCir46769.2022.9830516

Abstract

This paper presents an optically powered neural recording system for motor prediction using distributed free-floating motes. The proposed mote includes a neural recording amplifier, a data converter, feature extraction, and an on-chip antenna for implementing an RF uplink consuming only 42 nW. The entire mote IC dissipates 572 nW and occupies an area of 260×274 μm², representing the smallest neural recording system with RF uplink to date. Wireless and concurrent communication with multiple units is also demonstrated based on the code-division multiplexing.

Introduction

In the last decades, multiple wireless power and data transfer (WPDT) mechanisms have been explored for miniaturized neural probes. An RF-powered neural interface was presented in [1], however, it requires a relatively large 3×3 mm² antenna and the efficiency is limited to 3.4%. Ultrasound-based WPDT has the advantage of reduced absorption in human tissue, but it also requires a relatively large 0.8 mm³ transducer [2, 3]. Recently, an entirely optical WPDT system, powered by near infrared (NIR) light using a photovoltaic (PV) cell was proposed [4] and occupies an area of 190×280 μm². The two-way data telemetry is achieved using the PV cell (down-link and power) and an LED (uplink). However, the NIR-based wireless power transfer and data uplink introduce several challenges such as: (i) The LED requires a high-current pulse beyond the capability of the PV cell, thus a complex driver circuit is needed to slowly charge a capacitor and subsequently boost the voltage to drive the LED; (ii) Integrating an LED and a PV cell on the same GaAs substrate reduces the available area for the PV cell and limits the harvestable energy; (iii) Optical filters and two different wavelengths for the power and data telemetry are required to eliminate the interference from the power transfer. Alternatively, we find that an RF backscatter uplink is more compatible with optical power transfer by naturally decoupling the backward telemetry and power transmission through their disparate wavelengths. Further, RF backscatter has a simple and low power implementation on the mote side [5]. Key challenges associated with the RF backscatter arise from the small probe size, at < 500 μm, which causes a drastic reduction of magnetic coupling coefficient when the external unit is located at a cm-scale distance. However, by introducing a repeater unit (RU) in the epidural space (Fig. 1), the distance between the probe and the backscatter receiver can be kept to roughly 2 mm (dura thickness) allowing the miniaturization of the mote antenna.

In this work, we therefore propose an optical-RF neural probe using a 260×274 μm² on-chip antenna to implement a backscatter uplink, showing that near-field magnetic induction (NFMI) is a viable technique to communicate with microscale neural probes. To the best of the authors' knowledge, the proposed design represents the smallest neural recording unit featuring an RF uplink with on-chip antenna to date. The probe is optically powered by a PV cell to receive NIR light from the RU. The RU can independently address multiple probes using code-division multiple access, which is demonstrated with measurement results of a multi-channel backscatter communication.

Proposed Circuit

The envisioned system architecture is shown in Fig. 1. The probes use a carbon fiber electrode to sense neuron activity and are optically powered and programmed by the RU using NIR light at 850 μm wavelength. Each probe implements an RF uplink to communicate with the RU and encodes the transmitted signal with a pseudo-random chip ID. As a consequence, the repeater can detect the individual data by calculating code-domain correlation, as represented in Fig. 2. The RU is RF-powered by an external unit through NFMI. Fig. 3 shows the schematic of the neural recording chip. The signal chain consists of three main steps namely the signal acquisition, feature extraction, and data communication. An analog front-end (AFE) which includes amplifiers and an analog-to-digital converter (ADC) is used to amplify and digitize the input signal. The spiking band power (SBP), i.e., the average amplitude of the absolute signal in the frequency band from 300 Hz to 1 kHz, is then calculated for compression of the acquired signal, which is used for motor prediction with state-of-the-art accuracy [6]. The SBP calculation is accomplished by digitally integrating the AFE output and comparing it to a threshold. Finally, after each interval proportional to the calculated SBP, the switch for the on-chip antenna is triggered with its chip-ID to send a packet. The receiver chain is represented in Fig. 4 and is composed of a loop antenna, a directional coupler, a power detector, and a comparator. The loop antenna receives the backscatter signal, and the power detector performs envelope-based load-shift keying (LSK) demodulation. The carrier frequency is set to 3 GHz to ensure that the power consumed in the RU is lower than the safety limits while achieving a sufficient magnetic coupling. Fig. 5 shows the HFSS model and the simulated coupling coefficient as a function of the misalignment between the RU and the backscatter antenna. To achieve 10^{-6} BER at the repeater while consuming 1 mW, a coupling coefficient of 8×10^{-4} is required, while the proposed design achieved $> 2\times10^{-3}$ coupling coefficient in the area underneath the RU antenna. Fig. 6 shows the HFSS simulation results. At 3 GHz, the quality factors of the on-chip antenna and the RU antenna are 9 and 41, respectively. With a total power consumption of 0.87 mW, the communication system achieves a BER of 10^{-6}. Note that this power dissipated by a large RU (> 1cm²) satisfies the thermal limit of implanted devices (10 mW/cm²) [7].

Measurement Results

The proposed neural recording system was fabricated in a 180 nm CMOS process and occupies an area of 260×274 μm². The RF backscatter communication was tested with a 2×2 mm² loop antenna at a 2 mm distance. First, a single chip is characterized by applying spikes with different frequency and amplitude at its input terminals. The frequency and amplitude are swept from 25 Hz to 800 Hz and from 50 μV to 120 μV, respectively, as shown in Fig. 7(a) and (b). The packet rate varies accordingly from 1.2 Hz to 168 Hz in the amplitude sweep and from 0.8 Hz to 179 Hz in the frequency sweep, demonstrating a correct on-chip SBP calculation. The measured waveforms of the LSK demodulator output, matched filter output, and the recovered data are show in Fig. 7 (c). Second, simultaneous communication with multiple chips is demonstrated using 4 mote ICs and the results are compared with the single-channel case in Fig. 7. In the multi-channel experiment, each chip receives spikes with different amplitude and frequency to mimic the *in-vivo* measurement, so their symbol rates are different from each other. Then, the signal is demodulated using a matched filter for each chip ID in parallel. The recovered symbol rate is compared with the single-chip implementation showing good agreement as represented in Fig. 7(a) and (b). Transient waveforms of the received signal, matched filter output, and recovered data are shown in Fig. 7(d). Then, the SBP features are recovered from the output of the matched filters. Fig. 8(a) shows the SBP recovered from the RF communication (RF SBP) and the SBP calculated directly using the pre-recorded data from a monkey cerebral cortex (reference SBP). A Kalman filter, described in [6], is employed to decode finger position and velocity. The decoding is performed with 120 s of SBP from 20 channels. Fig. 8(b) shows the decoded position and velocity in the test set for both the RF SBP and reference SBP. The bottom-right table in Fig. 8 summarizes the decoding results. We demonstrate the comparable finger position decoding performance using RF SBP and reference SBP above 0.87 with a power consumption of 572 nW. Table I compares the proposed neural recording system with prior works.

References

[1] C. Kim, *et al.*, TBioCAS, 2019. [2] M. Ghanbari, *et al.*, ISSCC, 2019.
[3] D. Seo, *et al.*, Neuron, 2016. [4] J. Lim, *et al.*, VLSI, 2021.
[5] J. Rosenthal, *et. al.*, TBioCAS, 2019. [6] S. R. Nason, *et al.*, Nature BME, 2020.
[7] IEEE Standard for Safety Levels with Respect to Human Exposure to Radio Frequency Electromagnetic Fields, 3kHz to 300 GHz.

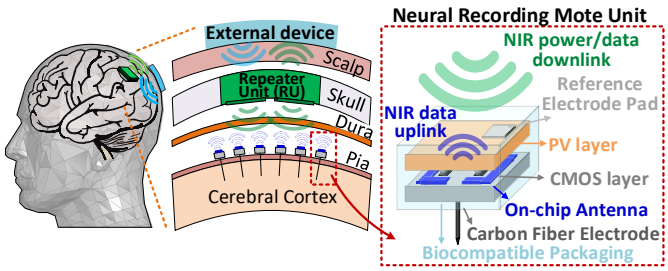

Fig. 1: System architecture of the proposed two-steps wireless neural recording system using optical NIR power and RF communication.

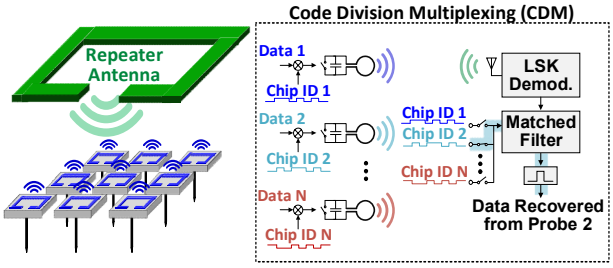

Fig. 2: Simplified schematic and operation of the proposed multi-antenna backscatter communication system using CDMA.

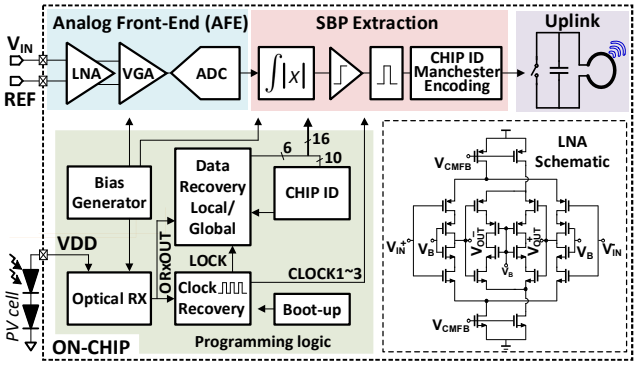

Fig. 3: Schematic of the proposed neural recording system including the AFE, the SBP extraction unit and the communication system.

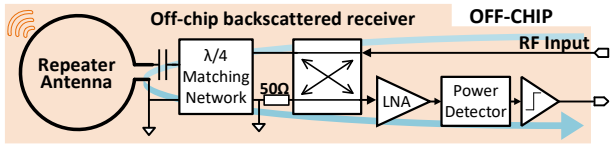

Fig. 4: Schematic of the backscatter receiver and LSK demodulator.

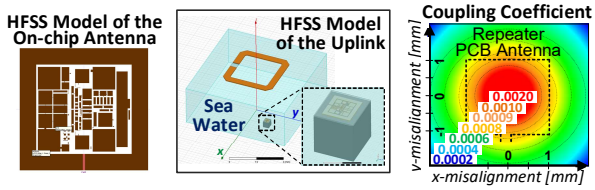

Fig. 5: HFSS model and simulated coupling coefficient of the on-chip antenna and uplink communication system in sea water environment.

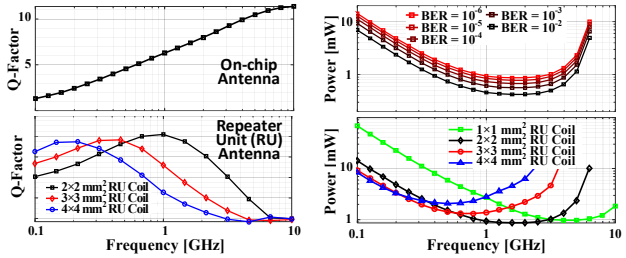

Fig. 6: Simulation results of the RF system, including the quality factors of the antennas, and estimated power consumption.

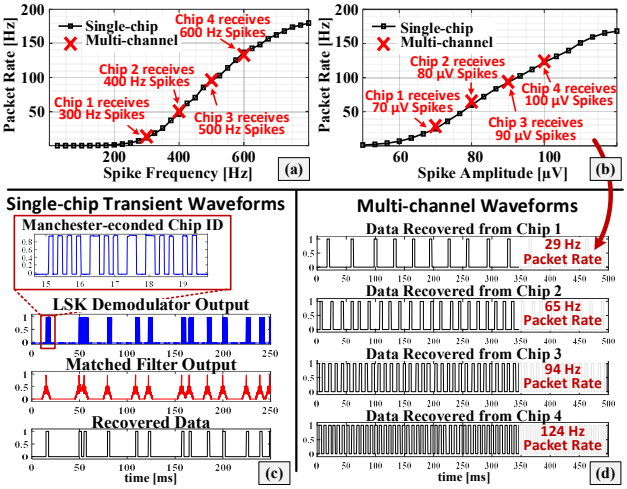

Fig. 7: Packet rate as a function of the spike amplitude and frequency when four chips are simultaneosly addressed using CDMA. The results are compared with measurements obtained from a single unit.

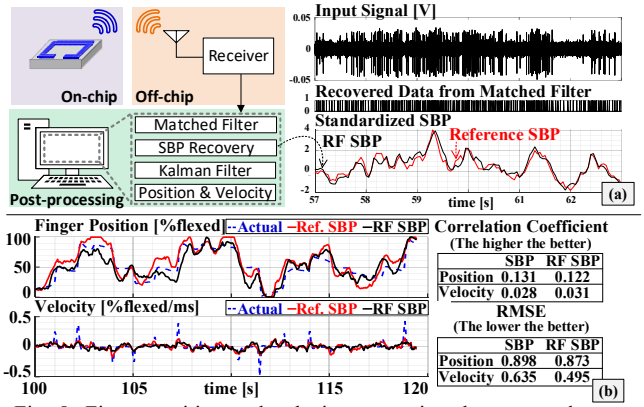

Fig. 8: Finger position and velocity comparing the proposed system with a reference SBP algorithm.

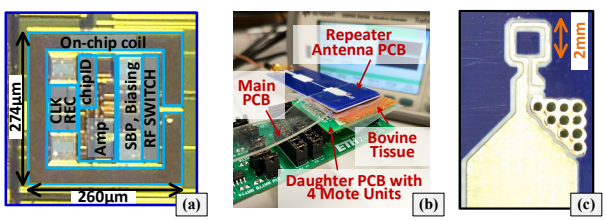

Fig. 9: Die micrograph (a), measurement setup (b) and repeater unit antenna, fabricated on a Rogers RO4003C substrate.

Table I: Performance Summary and Comparison

		JSSC 19'	TBioCAS18'	VLSI 21'	JPROC 17'	NER 19'	This Work
Technology [nm]		65	180	180	180	65	180
Wireless Method		Ultrasonic	Optical	Optical	RF	RF	RF
Chip area [mm²] (W [mm] x L [mm])		0.250 (0.50x0.50)	0.014 (0.25x0.06)	0.053 (0.19x0.28)	9 (3x3)	0.250 (0.50x0.50)	0.07 (0.26x0.27)
Data Link	Uplink	AM	PPM	PGM-SIM	LSK	RF	RF
	Downlink	No	No	PWM	ASK	ASK-PWM	Optical
Feature Extraction		No	No	SBP	No	No	SBP
Chip ID		Yes	No	Yes	No	Yes	Yes
Clock Recovery		No	No	Yes	No	No	Yes
Supply [V]		1	0.9	1.55	0.8	0.6	1.55
Power	Total [μW]	28.8	1	0.57*	<100	40	0.572
	Amplifier [μW]	4	0.5	0.36*	2	3.2	0.36
Target Neural Signal		LFP, AP	LPF, AP	AP	ECoG	ECoG	AP
Gain [dB]		24.0	30.0	67.2*	50-70	N/A	67.2*
Bandwidth [Hz]		5000	10000	[350, 1080]*	1000	500	[350, 1080]*

*Measured at 38°C